

“DARK” GRB 080325 IN A DUSTY MASSIVE GALAXY AT $z \sim 2^*$

T. Hashimoto¹, K. Ohta¹, K. Aoki², I. Tanaka², K. Yabe¹, N. Kawai³, W. Aoki⁴, H. Furusawa⁴, T. Hattori², M. Iye⁴, K. S. Kawabata⁵, N. Kobayashi⁶, Y. Komiyama⁴, G. Kosugi⁴, Y. Minowa², Y. Mizumoto⁴, Y. Niino¹, K. Nomoto⁷, J. Noumaru², R. Ogasawara⁴, T.-S. Pyo², T. Sakamoto⁸, K. Sekiguchi⁴, Y. Shirasaki⁴, M. Suzuki⁹, A. Tajitsu², T. Takata⁴, T. Tamagawa^{10,11}, H. Terada², T. Totani¹, J. Watanabe⁴, T. Yamada¹², and A. Yoshida¹³

ABSTRACT

We present optical and near infrared observations of *Swift* GRB 080325 classified as a “Dark GRB”. Near-infrared observations with Subaru/MOIRCS provided a clear detection of afterglow in K_s band, although no optical counterpart was reported. The flux ratio of rest-wavelength optical to X-ray bands of the afterglow indicates that the dust extinction along the line of sight to the afterglow is $A_V = 2.7 - 10$ mag. This large extinction is probably the major reason for optical faintness of GRB 080325. The $J - K_s$ color of the host galaxy, ($J - K_s = 1.3$ in AB magnitude), is significantly redder than those for typical GRB hosts previously identified. In addition to J and K_s bands, optical images in B , R_c , i' , and z' bands with Subaru/Suprime-Cam were obtained at about one year after the burst, and a photometric redshift of the host is

*Based on data collected at Subaru Telescope, which is operated by the National Astronomical Observatory of Japan.

¹Department of Astronomy, Kyoto University, Kyoto 606-8502, Japan

²Subaru Telescope, National Astronomical Observatory of Japan, 650 North A’ohoku Place, Hilo, HI 96720, USA

³Department of Physics, Tokyo Institute of Technology, 2-12-1 Ookayama, Meguro-ku, Tokyo 152-8551, Japan

⁴National Astronomical Observatory of Japan, 2-21-1 Osawa, Mitaka, Tokyo 181-8588, Japan

⁵Hiroshima Astrophysical Science Center, Hiroshima University, Higashi-Hiroshima, Hiroshima 739-8526, Japan

⁶Institute of Astronomy, University of Tokyo, 2-21-1 Osawa, Mitaka, Tokyo 181-0015, Japan

⁷Institute for the Physics and Mathematics of the Universe (IPMU), University of Tokyo, 5-1-5 Kashiwanoha, Kashiwa, Chiba 277-8568, Japan

⁸NASA Goddard Space Flight Center, Greenbelt, MD 20771, USA

⁹ISS Science Project Office, ISAS, JAXA, 2-1-1 Sengen, Tsukuba, Ibaraki 305-8505, Japan

¹⁰Department of Physics, Tokyo University of Science, 1-3 Kagurazaka, Shinjuku-ku, Tokyo 162-8601, Japan

¹¹Cosmic Radiation Laboratory, Institute of Physical and Chemical Research, 2-1 Hirosawa, Wako, Saitama 351-0198, Japan

¹²Astronomical Institute, Tohoku University, Sendai 980-8578, Japan

¹³Department of Physics, Aoyama Gakuin University, Sagami-hara, Kanagawa 229-8558, Japan

estimated to be $z_{photo} = 1.9$. The host luminosity is comparable to L^* at $z \sim 2$ in contrast to the sub- L^* property of typical GRB hosts at lower redshifts. The best-fit stellar population synthesis model for the host shows that a large dust extinction ($A_V = 0.8$ mag) attributes to the red nature of the host and that the host galaxy is massive ($M_* = 7.0 \times 10^{10} M_\odot$) which is one of the most massive GRB hosts previously identified. By assuming that the mass-metallicity relation for star-forming galaxies at $z \sim 2$ is applicable for the GRB host, this large stellar mass suggests the high metallicity environment around GRB 080325, consistent with inferred large extinction.

Subject headings: galaxies: photometry — gamma rays: burst

1. INTRODUCTION

The origin of a “dark” gamma-ray burst (GRB) remains one of the most serious mysteries of long GRB (hereafter just referred as GRBs) phenomena. A dark GRB is characterized by the faintness of its optical afterglow. While the X-ray afterglow is currently well-explored since the launch of *Swift*, an optical and/or near-infrared detection is reported in only about half of cases, suggesting the significant fraction of dark events. This optically dark nature may be attributed to the (i) large dust extinction around a GRB, (ii) attenuation by the neutral hydrogen in the host and/or intergalactic medium due to a high redshift event, (iii) intrinsically low luminous event of a small GRB fluence, and (iv) low-density medium surrounding a GRB progenitor. However, the actual nature of dark GRBs has not yet been revealed well.

Recently, the metallicity environment of dark GRBs is getting a lot more attention. The low metallicity has been theoretically suggested to be required to produce the rapid rotating progenitors and relativistic explosions associated with GRBs (Woosley & Bloom 2006; Yoon et al. 2006). As for observational studies, Fruchter et al. (2006) showed that GRBs preferentially occur in small faint irregular galaxies. This suggests the low-metallicity environment around GRBs because mass (or luminosity)-metallicity relation exists among galaxies. In fact, the low-metallicity nature of GRB hosts based on spectroscopic observations are reported by Stanek et al. (2006). Modjaz et al. (2008) compared the chemical abundances at the sites of 12 nearby ($z < 0.14$) type Ic supernovae (SN Ic) that showed broad lines, but had no observed gamma-ray burst (GRB), with the chemical abundances in five nearby ($z < 0.25$) galaxies at the sites of GRBs. They showed that there is a critical metallicity below which GRBs occur in contrast to type Ic SNe, which occur in more metal rich environment. In this context, Kocevski et al. (2009) predicted the critical stellar mass of GRB hosts, which is a stellar-mass counterpart of the critical metallicity, as a function of redshift, assuming an evolution of the mass-metallicity relation by Savaglio et al. (2005) and the presence of the critical metallicity (Modjaz et al. 2008). They showed that most GRB hosts collected by Savaglio et al. (2009) have stellar masses smaller than or comparable to the critical mass. There are, however, exceptionally massive hosts at $z \gtrsim 0.4$, i.e., possibly exceptionally high metallicity:

hosts of GRB 020127 ($z \sim 2$: Berger et al. 2007), GRB 020819, and GRB 051022 ($z = 0.4$ and 0.8 , respectively: Savaglio et al. 2009). For GRB 020819, Levesque et al. (2010) reported metallicity larger than the critical metallicity at the GRB position as well as in the host. In addition, for GRB 051022 metallicity of the host is slightly larger than the critical value above mentioned (Graham et al. 2009). Both GRBs are classified as dark¹. This suggests that high metallicity environment around a GRB may be somehow related to its “dark” nature. Therefore, investigating the properties of massive dark GRB hosts is a key to reveal the origin of dark GRBs.

The *Swift* Burst Alert Telescope (BAT) detected the long-duration GRB 080325 ($T_{90} = 128.4 \pm 34.2$ s) on 2008 March 25 at 04:10:32 UT with an initial localization of $3'$ radius (Vetere et al. 2008). The *Swift* X-Ray Telescope (XRT) began observing the field at 151.9 s after the BAT trigger, and found a bright, uncatalogued X-ray source (Vetere et al. 2008). The enhanced XRT position was reported by Osborne et al. (2008) by using 199 s of overlapping XRT Photon Counting mode with an uncertainty of $2''.6$ radius. After the trigger, several attempts were made to identify the afterglow in optical and near-infrared wavelength (de Ugarte Postigo et al. 2008; Brown & Vetere 2008; Clemens et al. 2008; Kudou et al. 2008; Im et al. 2008; Munz et al. 2008). However, no detection of the afterglow or host galaxy has been reported in optical and near-infrared wavelength, suggesting that the GRB 080325 is a dark GRB. In this paper we report the successful photometric identification of the afterglow of GRB 080325 in near-infrared wavelength and its host galaxy at $z \sim 2$, and present a case study of properties of the afterglow and its host galaxy of a dark GRB. This paper is organized as follows: in §2 the near-infrared and optical observations and data analysis are presented. In §3 we show the faintness of the optical and near-infrared afterglow of GRB 080325 compared with its X-ray afterglow, and dust extinction along the line of sight to GRB 080325. Results of spectral energy distribution fitting analysis of the GRB 080325 host and discussion are presented in §4 and §5, respectively.

Throughout this paper we use the AB magnitude system and the cosmological parameters of $H_0 = 71$ km s⁻¹ Mpc⁻¹, $\Omega_M = 0.27$, and $\Omega_\Lambda = 0.73$.

2. NEAR-INFRARED AND OPTICAL IMAGING WITH SUBARU

We observed the GRB 080325 field as a part of a target-of-opportunity program with the Subaru telescope. We took images of the field using Multi-Object InfraRed Camera and Spectrograph (MOIRCS) in J and K_s bands at 8.7 hours after the burst and another set at a day latter. A standard dithering method was employed during the exposure, with a single exposure of 50 s \times 2 coadds (first night) and 40 s \times 2 coadds (second night) in K_s band, and with 90 s (first night) and 150 s (second night) in J band. Total exposure times in J and K_s bands are 900 s and 3300 s for

¹It is not clear whether GRB 020127 is classified as “dark” or not because of no strong constraint on optical-to-X-ray spectral index of the afterglow ($\beta_{\text{OX}} < 1.24$: Jakobsson et al. 2004).

the first night, and 2250 s and 5040 s for the second night, respectively. The weather condition was clear for both nights. Seeing sizes were roughly $0''.6$ in K_s band and $0''.8$ in J band. A standard star field (FS27) was also observed during the first night at the end of the observation. The data reduction was performed with the MCSRED package (ver.20080317) using all-in-one task (mcsall).

We detected a faint extended object as well as a point-like spot at the northern edge of it in the enhanced *Swift* XRT error circle (Osborne et al. 2008) in the first-night K_s -band image as shown in Figure 1 (a). In the first-night J -band image, although the faint extended object was seen, the northern source was not detected. In the second-night K_s -band image, the north spot was not detected significantly as shown in Figure 1 (b). By subtracting the second image from the first image, the point-like spot can be isolated clearly (Figure 1(c)); a total magnitude (the spot and the extended object) decreased by 0.2 mag. No significant variation was detected in J band. Based on the positional coincidence, the FWHM of the northern spot comparable to a seeing size, and its fading behavior in K_s -band, we conclude that the spot in the north is the afterglow. The coordinates of the afterglow are $\alpha = 18^h31^m34^s.23$ and $\delta = +36^\circ31'24''.8$ (J2000, uncertainty $0''.2$). The aperture ($1''.2 \phi$) magnitudes of the afterglow at 8.7 hours after the burst are $J > 22.2$ mag and $K_s = 23.4 \pm 0.18$ mag. We also conclude that the faint extended source just south of the afterglow is the host galaxy of GRB 080325. The aperture ($2''.0 \phi$) magnitudes of the host galaxy are $J = 23.0 \pm 0.18$ mag and $K_s = 21.7 \pm 0.06$ mag. These magnitudes substantially represent total magnitudes because of convergence of growth curves at the aperture size of $2''.0$ in J and K_s bands. The offset distance of the afterglow from the galaxy center ($\delta r = 0''.8 = 7$ kpc) is large among other long GRBs, although the offset distance normalized by the half light radius of the host ($\delta r/r_e = 1.3$) is a typical value (Bloom et al. 2002; Fong et al. 2010). It should be mentioned here that probabilities of a chance coincidence of a foreground/background galaxy are small; the expected numbers of galaxies brighter than the magnitudes within $r \sim 1''.0$ from the position of the afterglow are $\sim 0.03 - 0.04$ in optical bands and ~ 0.01 in K_s -band (Metcalf et al. 2001; Rovilos et al. 2009; Cristóbal-Hornillos et al. 2003).

We obtained optical images of the GRB 080325 host with Subaru/Suprime-Cam in B , R_c , i' , and z' bands on 2009 April 22 (B , R_c , and z') and 2009 July 17 UT (i') to reveal the host properties. The total exposure times for B , R_c , i' , and z' bands are 900 s, 360 s, 360 s, and 1200 s, respectively. The weather condition was photometric and a typical seeing size was about $0''.6$ nearly identical to that of near-infrared images. The standard data reduction was performed for all images, i.e., bias subtraction, flat fielding, distortion correction, and sky subtraction using SDFRED package constructed by Yagi et al. (2002) and Ouchi et al. (2004). The images were calibrated with observations of SA111 standard stars (Landolt 2009). Obtained images are shown in Figure 2. We successfully detected the host galaxy with $B = 25.7 \pm 0.11$ mag, $R_c = 25.5 \pm 0.16$ mag, $i' = 24.9 \pm 0.16$ mag, and $z' = 24.5 \pm 0.07$ mag derived by aperture photometry using a $2''.0$ aperture size. The magnitude error includes a photometric error of the host galaxy calculated by IRAF phot task and a systematic error of a zero point in each band. All magnitudes described above are corrected for the foreground extinction by Milky Way (Schlegel et al. 1998).

3. GRB 080325 AS A DARK GRB

No optical and near-infrared detection of the afterglow has been reported other than our detection (Tanaka et al. 2008). This may indicate that GRB 080325 is a dark GRB. The definition of dark GRBs based only on the optical faintness of afterglow, however, is relatively unphysical since the optical detectability of an afterglow strongly depends on instruments, weather conditions, and starting time of follow-up observations. Thus Jakobsson et al. (2004) proposed a criterion based on an optical-to-X-ray spectral index at 11 hours after the burst, i.e., $\beta_{\text{OX}} = \log \{f_{\nu}(\text{R})/f_{\nu}(3 \text{ keV})\}/\log (\nu_{3\text{keV}}/\nu_{\text{R}})$. If β_{OX} of an afterglow is below 0.5, the GRB is defined as “dark”. In the simplest fireball models which have been successfully used to interpret the observed properties of GRB afterglows (Wijers et al. 1997; Sari et al. 1998), β_{OX} is expected to be $0.5 < \beta_{\text{OX}} < 1.25$. In fact, most of afterglows show β_{OX} between 0.5 to 1.25 as seen in Figure 3. The β_{OX} index would be little affected by the density of the GRB environment and the GRB luminosity. This is because these two cases tend to uniformly scale an overall spectrum of an afterglow, resulting in a nearly unchanged β_{OX} value. Based on the X-ray light-curve and spectral analyses of the GRB 080325 reported in *Swift*/XRT GRB light curve² and spectral³ repository, the X-ray flux in a 0.3 – 10 keV band at 11 hours was converted to the flux density at 3 keV using the measured X-ray spectral index of β_{X} . To estimate the *R*-band flux density of the afterglow at 11 hours, we assumed two possible cases of temporal declining index ($f_{\nu} \propto t^{-1.0}$ and $t^{-1.5}$) indicated by X-ray light curve of the afterglow (Evans et al. 2007). These indices well agree with a typical index of other X-ray afterglows. By using these temporal indices, the *I*-band upper limit measured with the 1.5m telescope at Sierra Nevada Observatory at 39.46 minutes after the burst (de Ugarte Postigo et al. 2008) is extrapolated to two upper limits at 11 hours. These *I*-band upper limits are extrapolated to *R*-band upper limits assuming a typical optical spectral index of $\beta_{\text{O/NIR}} = 1.0$. As a result, two upper limits on β_{OX} is estimated to be 0.14 and 0.33 (Figure 3). We also confirmed the power-law interpolations between *I*-band upper limits and K_s band flux densities at 11 hours result in β_{OX} slightly smaller than these values, assuming above two temporal declining indices (the power-law indices in this interpolation are $\beta_{\text{O/NIR}} = 1.6$ and 2.9 for t^{-1} and $t^{-1.5}$). Therefore, GRB 080325 is classified as a dark GRB.

Given a typical optical spectral index of $\beta_{\text{O/NIR}} = 1.0$ and the observed K_s magnitude of the afterglow, the expected *J*-band magnitude of the afterglow at the first night is estimated to be $J = 24.0$ mag, which is fainter than the *J*-band limiting magnitude of the first-night image. This result is unchanged even if two power-law indices of $\beta_{\text{O/NIR}} = 1.6$ and 2.9 mentioned above are assumed. Therefore, it is unclear whether large attenuation by dust or intergalactic medium are present or not from the $J - K_s$ color of the afterglow. Another method to examine the attenuation along the line of sight to the GRB is a comparison between flux densities of the X-ray and optical afterglows. As mentioned above, “intrinsic”(rest-wavelength obscuration-free) optical-to-X-ray spectral index

²http://www.swift.ac.uk/xrt_curves/

³http://www.swift.ac.uk/xrt_spectra/

($\beta_{\text{OX,int}}$) is expected to be 0.5 - 1.25. If we estimate the “intrinsic” 3 keV flux density of the afterglow ($f_{3\text{keV,int}}$), a possible range of the “intrinsic” R -band flux density ($f_{R,int}$) can be obtained. Thus, the comparison between $f_{R,int}$ and observed rest-wavelength R -band flux density of the afterglow ($f_{R,obs}$) enables us to estimate an extinction along the line of sight to the GRB. So as to estimate a possible range of $f_{R,int}$, we obtained the X-ray spectrum of the GRB 080325 afterglow averaged from 1 to 16 hours after the burst from the Swift/XRT GRB spectral repository, and performed spectral fitting analysis as shown in Figure 4. The X-ray spectral model includes a fixed extinction by Milky Way ($N_{\text{H}} = 3.8 \times 10^{20} \text{ cm}^{-2}$), an extinction to the afterglow of GRB 080325 at $z = 1.9$ ($N_{\text{H,AG}}$), and a power-law X-ray spectral index of β_{X} . The redshift of the afterglow assumed here is based on spectral energy distribution (SED) fitting analysis for the host galaxy described in section 4. Using the derived best-fit parameters of $N_{\text{H,AG}} = (1.8^{+0.8}_{-0.6}) \times 10^{22} \text{ cm}^{-2}$ and $\beta_{\text{X}} = 1.2^{+0.3}_{-0.2}$, the X-ray flux in a 0.3 – 10 keV band at 11 hours extracted from X-ray light curve was converted to $f_{3\text{keV,int}} = 0.20 \text{ } \mu\text{Jy}$. Based on $f_{3\text{keV,int}}$ and $\beta_{\text{OX,int}}$, we calculated a possible range of $f_{R,int}$. With the Calzetti extinction law (Calzetti et al. 2000), the extinction along the line of sight to the GRB is estimated to be $2.7 \text{ mag} < A_V < 10 \text{ mag}$. If extinction laws for Milky Way (Pei 1992) and SMC (Prevot et al. 1984; Bouchet et al. 1985) are assumed, the extinction is $2.8 \text{ mag} < A_V < 11 \text{ mag}$ for both cases. Since these values are corresponding to $\beta_{\text{OX,int}} = 0.5$ and 1.25, respectively, we can not exclude the extremely strong dust extinction of $A_V > 10 \text{ mag}$ if $\beta_{\text{OX,int}} > 1.25$ is possible, e.g., there is one exceptional object with $\beta_{\text{OX}} > 1.25$ as shown in Figure 3. As an alternative, the best-fit result of $N_{\text{H,AG}} = 1.8 \times 10^{22} \text{ cm}^{-2}$ can be converted to $A_V \sim 10$ assuming a typical ratio of A_V/N_{H} for the Local Group galaxies (Milky Way, SMC, and LMC: Schady et al. 2007). In any cases A_V along the line of sight to the GRB is larger than A_V for the entire host derived below.

4. MASSIVE RED HOST GALAXY AT $z \sim 2$

In order to estimate a redshift and to reveal host properties we made SED fitting for the host. The stellar properties of the GRB 080325 host are examined using the observed multi-band photometry and stellar population synthesis models including emission lines typical for local star-forming galaxies (PÉGASE.2) constructed by Fioc & Rocca-Volmerange (1997) and Fioc & Rocca-Volmerange (1999). Assumed star-formation histories (SFHs) include (i) instantaneous burst, (ii) exponentially declining star-formation rate (SFR), i.e., $e^{-\frac{t}{\tau}}$ with $\tau = 1 \text{ Myr}, 10 \text{ Myr}, 100 \text{ Myr}, 1 \text{ Gyr},$ and 10 Gyr , and (iii) constant SFR. The initial mass function (IMF) used here is Salpeter IMF (Salpeter 1955), and the extinction law is adopted from Calzetti et al. (2000). Although we also examined Milky Way and SMC extinction laws, these provided very poor fitting results. We used *SEDfit* software package (M. Sawicki 2010, in preparation) which is essentially the same as that by Sawicki & Yee (1998).

The SFH of the best-fit stellar population synthesis model is the τ ($= 1 \text{ Gyr}$) declining model ($\chi^2 = 5.4$), and the best-fit result and output parameters of the host galaxy are summarized in Figure 5. However $\tau = 10 \text{ Gyr}$ and constant SFR models can also reasonably reproduce the observed

SED ($\chi^2 = 7.8$). These models give that the host is at $z = 1.8 - 2.2$ with the best estimate of 1.9 (see Figure 6), and the dust extinction is large ($A_V = 0.8 - 1.6$ mag, $E(B - V) = 0.2 - 0.4$ mag). The $M_{*,\text{Salp}}$ (stellar mass for Salpeter IMF), SFR, and age of the host derived from SED fitting are $(1.2 - 1.8) \times 10^{11} M_\odot$, $10 - 80 M_\odot \text{ yr}^{-1}$, and $3.0 - 3.5$ Gyr, although uncertainties of the SFR and age are relatively large.

The rest-frame B -band absolute magnitude is $M_B = -21.8$ calculated from the best-fit spectral template. This magnitude is comparable to L^* at $1.8 < z < 2.0$ (Dahlen et al. 2005), or $3 L^*$ if the B -band luminosity is corrected for the dust extinction. As shown in Figure 7, the observed color of the GRB 080325 host ($J - K_s = 1.3$ mag) is significantly redder than any other GRB hosts (large blue dots with vertical error bars: Levan et al. 2006; Berger et al. 2007; Jaunsen et al. 2008; Savaglio et al. 2009) at $z \leq 2$, GOODS South galaxies with known spectroscopic redshifts (small black dots: Grazian et al. 2006) and local-galaxy templates (different line types: Coleman et al. 1980) redshifted to $z \sim 2$ without galaxy evolution except for an elliptical galaxy. These properties of the host galaxy, i.e., the luminous dusty (red-color) starforming host, are significantly different from those of typical GRB hosts previously studied by Le Floc'h et al. (2003). We note that these results do not change even if population synthesis models without including nebular emission lines are examined for the SED fitting analysis. Hereafter, we adopt parameters of the host galaxy derived from the best-fit model with emission lines.

5. COMPARISON WITH OTHER GRB AFTERGLOWS AND HOSTS

5.1. OPTICAL FAINTNESS DUE TO DUST EXTINCTION

Recently Perley et al. (2009) have made a uniform sample of dark GRBs. Among 29 GRB hosts rapidly observed with the Plomar 60-inch telescope from *Swift* burst, they selected 14 dark GRBs based on β_{OX} at 1000 s after the burst. They inferred that a significant fraction of dark GRBs occurs in highly obscured regions, although the host galaxies of dark GRBs seem to have normal optical colors. This suggests that the source of obscuring dust is local to the vicinity of the GRB progenitor or highly unevenly distributed within the host galaxy. Perley et al. (2009) demonstrated that the typical dust extinction along the line of sight to dark GRBs is $0.5 \text{ mag} < A_V < 10.0 \text{ mag}$. The dust extinction along the line of sight to GRB 080325 is similar to these values. However, GRB 080325 host is characteristic in the sense that the large extinction is observed both for the entire host and the line of sight to the GRB, in contrast to most of other dark GRBs which show relatively weak extinction for the whole host galaxies, i.e., $A_V < 0.5$ mag (Perley et al. 2009). Another case of dark GRB with a large extinction over the whole host galaxy, is GRB 051022. GRB 051022 is classified as dark with $\beta_{\text{OX}} < -0.05$, whose host galaxy shows a relatively large dust extinction of $A_V \sim 1.0$ mag derived from SED fitting analysis (Rol et al. 2007; Castro-Tirado et al. 2007). The amount of the extinction in the line of sight toward the GRB ($A_V = 4.4$ mag), which is required to suppress the optical afterglow to the observed limits, is clearly higher than the A_V value found

from the host SED. Rol et al. (2007) attributed this significant discrepancy between two values of the dust extinction to the effect of the GRB position in the host where the line of sight crosses a dense region in the host. As for GRB 080325, the dust extinction along the line of sight to the burst is larger than that for the host as a whole and the GRB is located at the outskirts of the host galaxy. Therefore, the local dusty environment such as circumstellar matter and/or molecular cloud around GRB 080325 is likely to be a major reason for the optical faintness of GRB 080325 relative to X-ray brightness rather than extinction by dust distributed over the entire host.

5.2. MASSIVE GRB HOST AND ORIGIN OF A DARK GRB

As mentioned in §4, the host of GRB 080325 is as luminous as L^* at $z \sim 2$. This property is also seen in the apparent K_s -band magnitude as shown in Figure 8. The host of GRB 080325 is located in the bright end of the apparent K_s magnitude distribution of the GOODS south galaxies at the same redshift range. It is contrary to the distribution of other GRB hosts, which are slightly fainter than that of the GOODS south galaxies. In this figure, the host of GRB 080325 is denoted by a red square. Previously identified GRB hosts with and without known redshift are shown by large blue dots and arrows (Chary et al. 2002; Le Floc’h et al. 2003; Levan et al. 2006; Berger et al. 2007; Jaunsen et al. 2008; Tanvir et al. 2008; Savaglio et al. 2009) and GOODS South field galaxies with spectroscopic redshifts are indicated by small black dots (Grazian et al. 2006). Black arrows represent extinction vectors for $A_V = 1.0$ mag at each redshift assuming the Calzetti extinction law (Calzetti et al. 2000). For comparison, tracks of model galaxies (τ declining models used in §4) with $M_K = -23$ mag and -20 mag without extinction are shown by the solid and dashed lines.

Figure 9 shows stellar masses of GRB hosts by Savaglio et al. (2009) (large blue dots), GOODS South galaxies by Grazian et al. (2006) (small black dots), and GRB 080325 host (a red dot) against redshift. Figure 9 clearly demonstrates that GRB 080325 host is one of the most massive GRB hosts ($M_{*,\text{BG}} = 7.0 \times 10^{10} M_\odot$, described below) among dark and non-dark GRB hosts previously identified. We note that the methods of the SED fitting analysis are, in some degree, different between GRB hosts by Savaglio et al. (2009) and other samples including GOODS South galaxies and GRB 080325 hosts. Savaglio et al. (2009) assumed the IMF by Baldry & Glazebrook (2003) and two stellar-population components, while our SED-fitting analysis for GRB 080325 host and GOODS South galaxies is based on Salpeter IMF and a single stellar-population component as described in §4. Thus, to examine the effect by using different methods, stellar masses of GRB hosts (except for hosts for which only two-band data are available) by Savaglio et al. (2009) were compared with those derived by our method. After the systematic difference between two IMFs is taken into account, i.e., a total stellar mass derived by Salpeter IMF is 1.8 times larger than that derived by using Baldry & Glazebrook (2003) IMF, we found that both stellar masses agree with each other within 1σ uncertainty of $\delta \log M_* = 0.4$. In Figure 9, $M_{*,\text{Salp}}$ of the GRB 080325 host and GOODS-South field galaxies are converted to $M_{*,\text{BG}}$ which is stellar mass derived by Baldry & Glazebrook (2003) IMF.

Since the stellar mass of the GRB 080325 host is large, the metallicity may exceed the critical metallicity suggested by Modjaz et al. (2008) below which GRBs ($z < 0.14$) occur. If we assume the mass-metallicity relations obtained for star-forming galaxies at $z \sim 2$ (Erb et al. 2006; Hayashi et al. 2009), the expected oxygen abundances (hereafter referred as metallicity) based on Kewley & Dopita (2002) method are $12 + \log (\text{O}/\text{H}) = 8.88$ or 9.06 . This expected metallicity of GRB 080325 host significantly exceeds the critical metallicity as shown in Figure 10. This suggests a high metallicity environment around GRB 080325.

Similarly, high metallicity environments of GRBs were recently reported for GRB 020819 and GRB 051022 by spectroscopic observations (Levesque et al. 2010; Graham et al. 2009). These GRBs commonly have massive hosts and are classified as dark. Thus, these three cases including GRB 080325 suggest the dusty high metallicity environment of GRBs. As one explanation, Levesque et al. (2010) suggest the possibility that the enhanced mass loss rates associated with higher metallicities could potentially contribute to large amount of circumburst extinction, i.e., to produce a dark GRB.

On the other hand, numerical calculations for a single star scenario of the GRB phenomenon suggest the low-metallicity environment around GRB progenitors is required (Woosley & Bloom 2006; Yoon et al. 2006). Thus the possible high metallicity environment around GRB 080325 seems to favor binary-star merger scenario (Nomoto et al. 1995; Fryer et al. 1999; Iwamoto et al. 2000). In this scenario, the merging stars take in their orbital angular momentum during the merging process. Therefore, the resulting collapsar can maintain a sufficient angular momentum required for a GRB explosion even if the high-metallicity environment. However, we note that the metallicity at the GRB position may be smaller than the critical metallicity, because of the metallicity gradient in the host (the position of GRB 080325 is at the edge of the host).

6. SUMMARY

We successfully detected an afterglow of GRB 080325 in K_s band at 8.7 hours after the burst and its host galaxy in K_s and J band with Subaru/MOIRCS although no optical counterpart was reported. GRB 080325 is classified as a “Dark GRB” based on optical-to-X-ray spectral index of $\beta_{\text{OX}} < 0.2 - 0.5$. The flux ratio of rest-wavelength optical to X-ray bands of the afterglow shows a very large dust extinction along the line of sight to the afterglow ($A_V = 2.7 - 10$ mag). To reveal host properties, we obtained optical images in B , R_c , i' , and z' bands with Subaru/Suprime-Cam at about one year after the burst, and clearly detected the host galaxy in these bands. The SED fitting analysis for the host galaxy was performed assuming the Calzetti et al. extinction law and various star formation histories including instantaneous, exponentially declining ($e^{-\frac{t}{\tau}}$ with $\tau = 1$ Myr, 10 Myr, 100 Myr, 1 Gyr, and 10 Gyr), and constant star formation rate. The best-fit stellar population synthesis model ($\tau = 1$ Gyr) indicates that the host is at $z_{\text{photo}} = 1.9$. The dust extinction for the entire host ($A_V = 0.8$ mag) is larger than those of typical GRB hosts. Although GRB 080325 is located at the outskirts of the host galaxy, the dust extinction along the line of sight to GRB 080325

is larger than that for the entire host. Therefore, a major reason for the optical faintness of GRB 080325 relative to X-ray brightness is likely attributed to the local dusty environment around GRB 080325 rather than extinction by dust distributed over the entire host. We found that the host is very luminous (comparable to L^* at $z \sim 2.0$) and very massive ($M_* = 7.0 \times 10^{10} M_\odot$) in contrast to the faint and less massive properties of GRB hosts at lower redshifts. Considering the mass-metallicity relation for star-forming galaxies at $z \sim 2$ and the stellar mass of the GRB 080325 host, the high metallicity environment around GRB 080325 is suggested. This possible high metallicity environment favors the binary merger scenario of the GRB phenomenon rather than the single star explosion, although the future spectroscopic observation at the GRB position is essential.

We are grateful to the Subaru Telescope staffs for conducting ToO and Service observations. We would also like to thank Fumiaki Nakata and Sakurako Okamoto for useful comments on data reduction and analysis. We also thank Marcin Sawicki for providing us the “*SEDfit*”. We would also like to thank the anonymous referee for his/her comments which improved the paper. This work is supported by the Grant-in-Aid for Scientific Research Priority Areas (19047003) and the Grant-in-Aid for the Global COE Program ”The Next Generation of Physics, Spun from Universality and Emergence” from the Ministry of Education, Culture, Sports, Science and Technology (MEXT) of Japan.

REFERENCES

- Baldry, I. K., & Glazebrook, K. 2003, *ApJ*, 593, 258
- Berger, E., Fox, D. B., Kulkarni, S. R., Frail, D. A., & Djorgovski, S. G. 2007, *ApJ*, 660, 504
- Bloom, J. S., Kulkarni, S. R., & Djorgovski, S. G. 2002, *AJ*, 123, 1111
- Bouchet, P., Lequeux, J., Maurice, E., Prevot, L., & Prevot-Burnichon, M. L. 1985, *A&A*, 149, 330
- Brown, P. J., & Vetere, L. 2008, *GCN Circular*, 7518, 1
- Bruzual A., G., & Charlot, S. 1993, *ApJ*, 405, 538
- Calzetti, D. 1997, *AJ*, 113, 162
- Calzetti, D., Armus, L., Bohlin, R. C., Kinney, A. L., Koornneef, J., & Storchi-Bergmann, T. 2000, *ApJ*, 533, 682
- Castro-Tirado, A. J., et al. 2007, *A&A*, 475, 101
- Chary, R., Becklin, E. E., & Armus, L. 2002, *ApJ*, 566, 229
- Clemens, C., Yoldas, A. K., Greiner, J., Yoldas, A., Kruehler, T., & Szokoly, G. 2008, *GCN Circular*, 7520, 1

- Coleman, G. D., Wu, C.-C., & Weedman, D. W. 1980, *ApJS*, 43, 393
- Cristóbal-Hornillos, D., Balcells, M., Prieto, M., Guzmán, R., Gallego, J., Cardiel, N., Serrano, Á., & Pelló, R. 2003, *ApJ*, 595, 71
- Dahlen, T., Mobasher, B., Somerville, R. S., Moustakas, L. A., Dickinson, M., Ferguson, H. C., & Giavalisco, M. 2005, *ApJ*, 631, 126
- de Ugarte Postigo, A., Sota, A., Gorosabel, J., & Castro-Tirado, A. J. 2008, *GCN Circular*, 7516, 1
- Erb, D. K., Shapley, A. E., Pettini, M., Steidel, C. C., Reddy, N. A., & Adelberger, K. L. 2006, *ApJ*, 644, 813
- Evans, P. A., et al. 2007, *A&A*, 469, 379
- Fioc, M., & Rocca-Volmerange, B. 1997, *A&A*, 326, 950
- Fioc, M., & Rocca-Volmerange, B. 1999, *arXiv:astro-ph/9912179*
- Fong, W., Berger, E., & Fox, D. B. 2010, *ApJ*, 708, 9
- Fruchter, A. S., et al. 2006, *Nature*, 441, 463
- Fryer, C. L., Woosley, S. E., & Hartmann, D. H. 1999, *ApJ*, 526, 152
- Graham, J. F., Fruchter, A. S., Kewley, L. J., Levesque, E. M., Levan, A. J., Tanvir, N. R., Reichart, D. E., & Nysewander, M. 2009, *American Institute of Physics Conference Series*, 1133, 269
- Grazian, A., et al. 2006, *A&A*, 449, 951
- Hayashi, M., et al. 2009, *ApJ*, 691, 140
- Im, M., Lee, I., & Urata, Y. 2008, *GCN Circular*, 7529, 1
- Iwamoto, K., et al. 2000, *ApJ*, 534, 660
- Jakobsson, P., Hjorth, J., Fynbo, J. P. U., Watson, D., Pedersen, K., Björnsson, G., & Gorosabel, J. 2004, *ApJ*, 617, L21
- Jaunsen, A. O., et al. 2008, *ApJ*, 681, 453
- Kewley, L. J., & Dopita, M. A. 2002, *ApJS*, 142, 35
- Kewley, L. J., & Ellison, S. L. 2008, *ApJ*, 681, 1183
- Kocevski, D., West, A. A., & Modjaz, M. 2009, *ApJ*, 702, 377
- Kudou, Y., Shimokawabe, T., & Kawai, N. 2008, *GCN Circular*, 7522, 1

- Landolt, A. U. 2009, *AJ*, 137, 4186
- Le Floc'h, E., et al. 2003, *A&A*, 400, 499
- Levan, A., et al. 2006, *ApJ*, 647, 471
- Levesque, E. M., Kewley, L. J., Graham, J. F., & Fruchter, A. S. 2010, *ApJ*, 712, L26
- Metcalf, N., Shanks, T., Campos, A., McCracken, H. J., & Fong, R. 2001, *MNRAS*, 323, 795
- Modjaz, M., et al. 2008, *AJ*, 135, 1136
- Munz, F., et al. 2008, *GCN Circular*, 7563, 1
- Nomoto, K. I., Iwamoto, K., & Suzuki, T. 1995, *Phys. Rep.*, 256, 173
- Osborne, J. P., Beardmore, A. P., Evans, P. A., & Goad, M. R. 2008, *GCN Circular*, 7513, 1
- Ouchi, M., et al. 2004, *ApJ*, 611, 660
- Pei, Y. C. 1992, *ApJ*, 395, 130
- Perley, D. A., et al. 2009, *AJ*, 138, 1690
- Prevot, M. L., Lequeux, J., Prevot, L., Maurice, E., & Rocca-Volmerange, B. 1984, *A&A*, 132, 389
- Rol, E., et al. 2007, *ApJ*, 669, 1098
- Rovilos, E., et al. 2009, *A&A*, 507, 195
- Salpeter, E. E. 1955, *ApJ*, 121, 161
- Sari, R., Piran, T., & Narayan, R. 1998, *ApJ*, 497, L17
- Savaglio, S., et al. 2005, *ApJ*, 635, 260
- Savaglio, S., Glazebrook, K., & LeBorgne, D. 2009, *ApJ*, 691, 182
- Sawicki, M., & Yee, H. K. C. 1998, *AJ*, 115, 1329
- Schady, P., et al. 2007, *MNRAS*, 377, 273
- Schlegel, D. J., Finkbeiner, D. P., & Davis, M. 1998, *ApJ*, 500, 525
- Stanek, K. Z., et al. 2006, *Acta Astronomica*, 56, 333
- Tanaka, I., Pyo, T.-S., Hattori, T., Aoki, K., Tokoku, C., Yamada, T., Ohta, K., & Kawai, N. 2008, *GCN Circular*, 7524, 1
- Tanvir, N. R., et al. 2008, *MNRAS*, 388, 1743

- van der Horst, A. J., Kouveliotou, C., Gehrels, N., Rol, E., Wijers, R. A. M. J., Cannizzo, J. K., Racusin, J., & Burrows, D. N. 2009, *ApJ*, 699, 1087
- Vetere, L., et al. 2008, *GCN Circular*, 7512, 1
- Wijers, R. A. M. J., Rees, M. J., & Meszaros, P. 1997, *MNRAS*, 288, L51
- Woosley, S. E., & Bloom, J. S. 2006, *ARA&A*, 44, 507
- Yagi, M., Kashikawa, N., Sekiguchi, M., Doi, M., Yasuda, N., Shimasaku, K., & Okamura, S. 2002, *AJ*, 123, 66
- Yoon, S.-C., Langer, N., & Norman, C. 2006, *A&A*, 460, 199
- Zheng, W.-K., Deng, J.-S., & Wang, J. 2009, *Research in Astronomy and Astrophysics*, 9, 1103

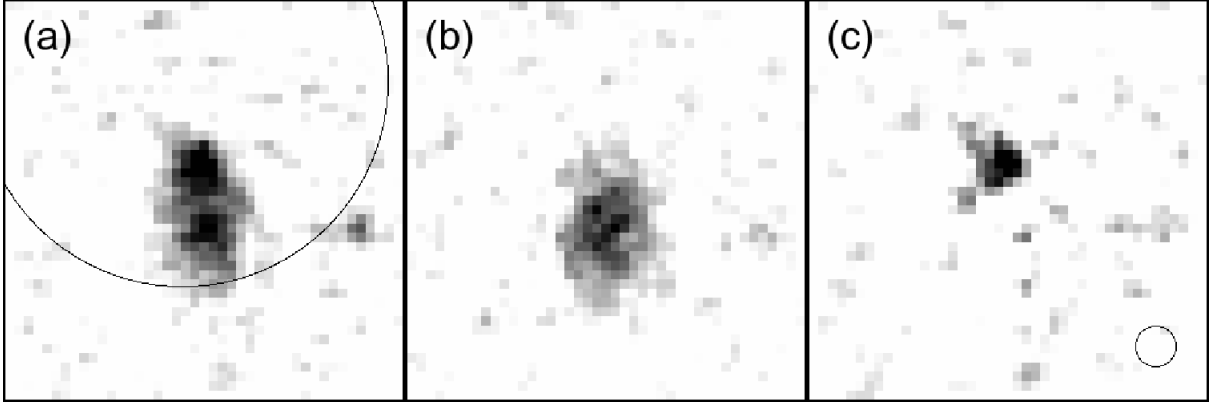


Fig. 1.— K_s band images ($5''.0 \times 5''.0$) of GRB 080325 host galaxy at 8.7 hours (a), and 33.5 hours (b) after the burst. (c) Subtracted image. North is up and east is to left. Large and small circles represent the enhanced *Swift* XRT error circle (Osborne et al. 2008) and a seeing size of $\sim 0''.5$, respectively.

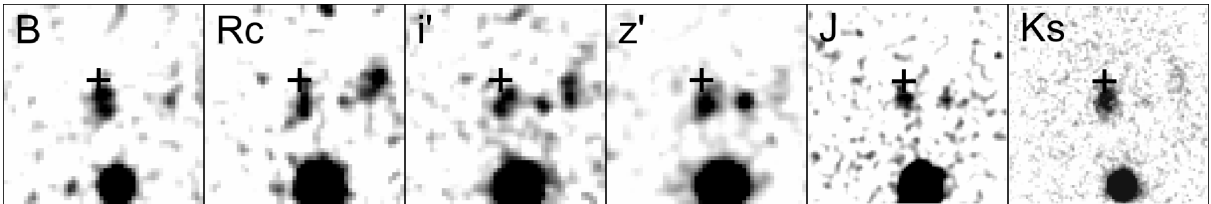


Fig. 2.— Optical-to-near-infrared images ($10''.0 \times 10''.0$) of the GRB host galaxy obtained by Subaru/Suprime-Cam and MOIRCS. North is up and east is to left. Cross shows the position of the GRB 080325 afterglow detected in K_s band.

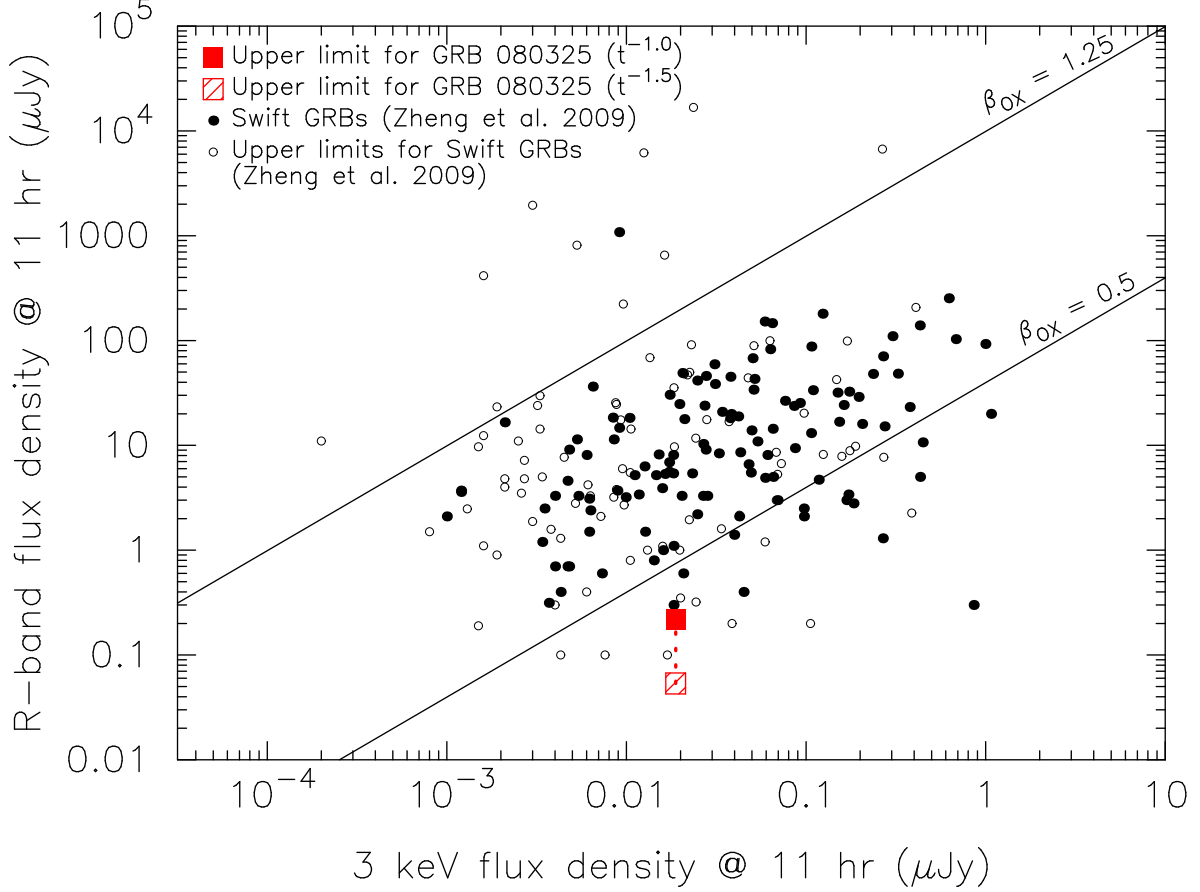


Fig. 3.— R -band flux density versus 3 keV X-ray flux density at 11 hours after the burst for long GRBs (Zheng et al. 2009). Filled and open circles refer to optical detections reported and optical upper limits, respectively. Two solid lines show the theoretical limiting values of $\beta_{\text{OX}} = 0.5$ and 1.25 . Estimated two upper limits on R -band flux densities of the GRB 080325 afterglow are plotted by red filled ($t^{-1.0}$) and hatched ($t^{-1.5}$) squares connected by a dotted line.

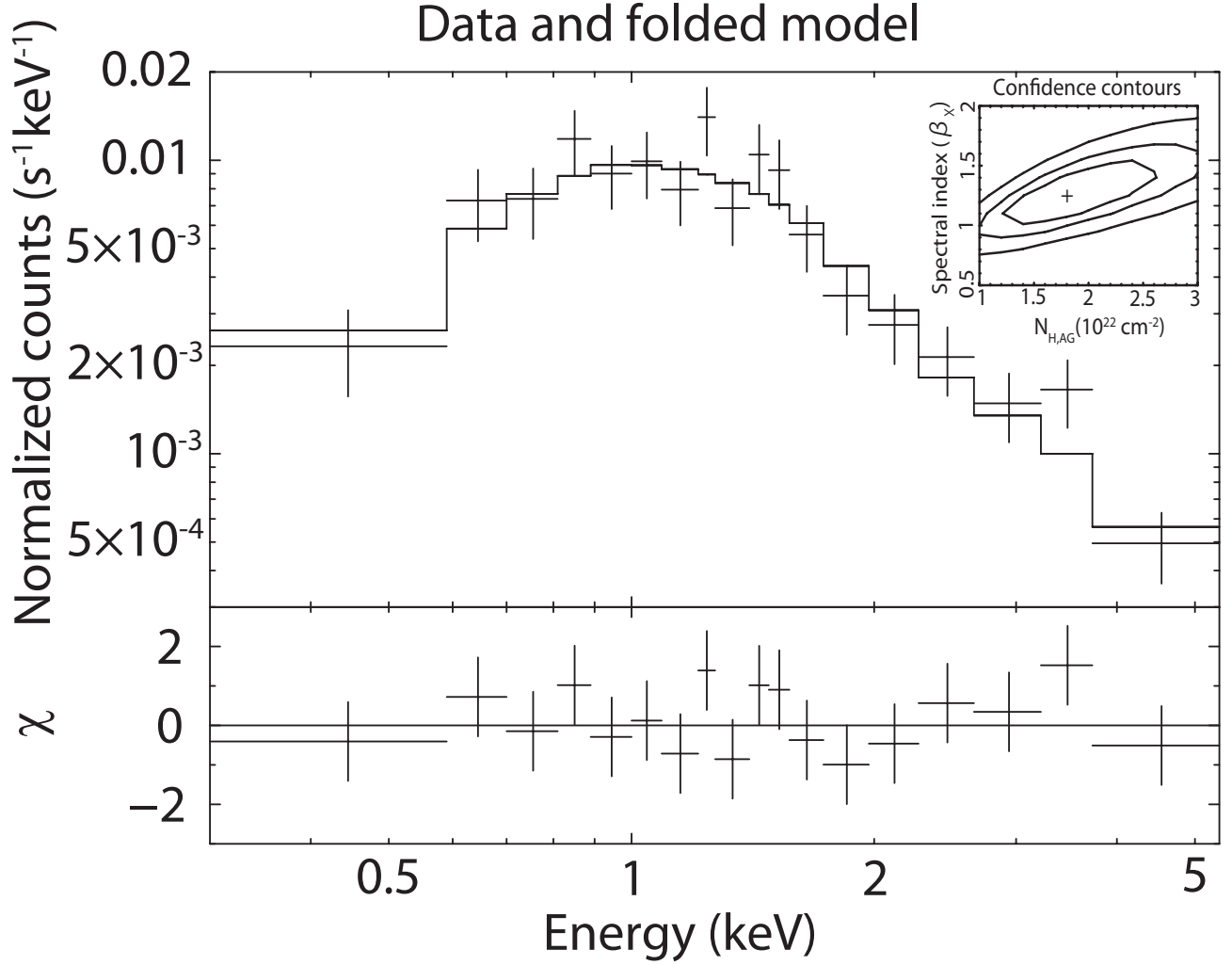


Fig. 4.— (Top) Observed spectrum of the X-ray afterglow averaged from 1 to 16 hours after the burst and the best-fit spectral model (solid line). Inserted three contours indicate 68%, 90%, and 99% confidence levels in the parameter space of β_X and $N_{\text{H,AG}}$, and a central cross is best-fit result. (Bottom) Delta chi-square at each energy bin.

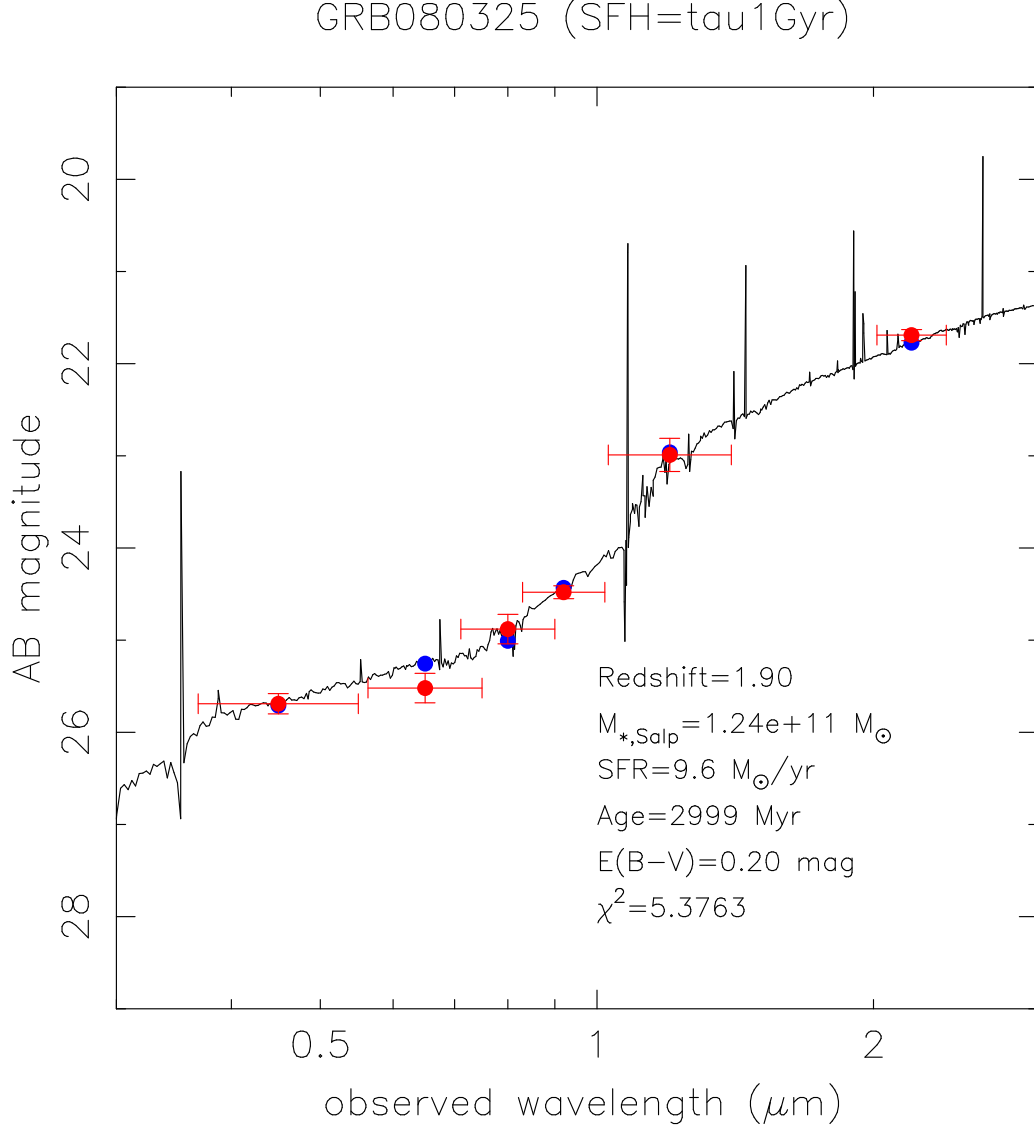


Fig. 5.— Observed SED of the GRB 080325 host galaxy (red dots with error bars) and the best-fit synthetic spectrum (black solid line) with PÉGASE.2, which is a code to compute the galaxy stellar population synthesis models including emission lines from ionized gas (Fioc & Rocca-Volmerange 1997, 1999). Blue dots without error bars show AB magnitude of the best-fit model in observed bands. The best-fit model shows the dusty ($E(B-V) = 0.2 \text{ mag}$) massive ($M_{*,\text{Salp}} = 1.24 \times 10^{11} M_{\odot}$) starforming ($\text{SFR} = 9.6 M_{\odot} \text{ yr}^{-1}$) host galaxy at $z = 1.9$.

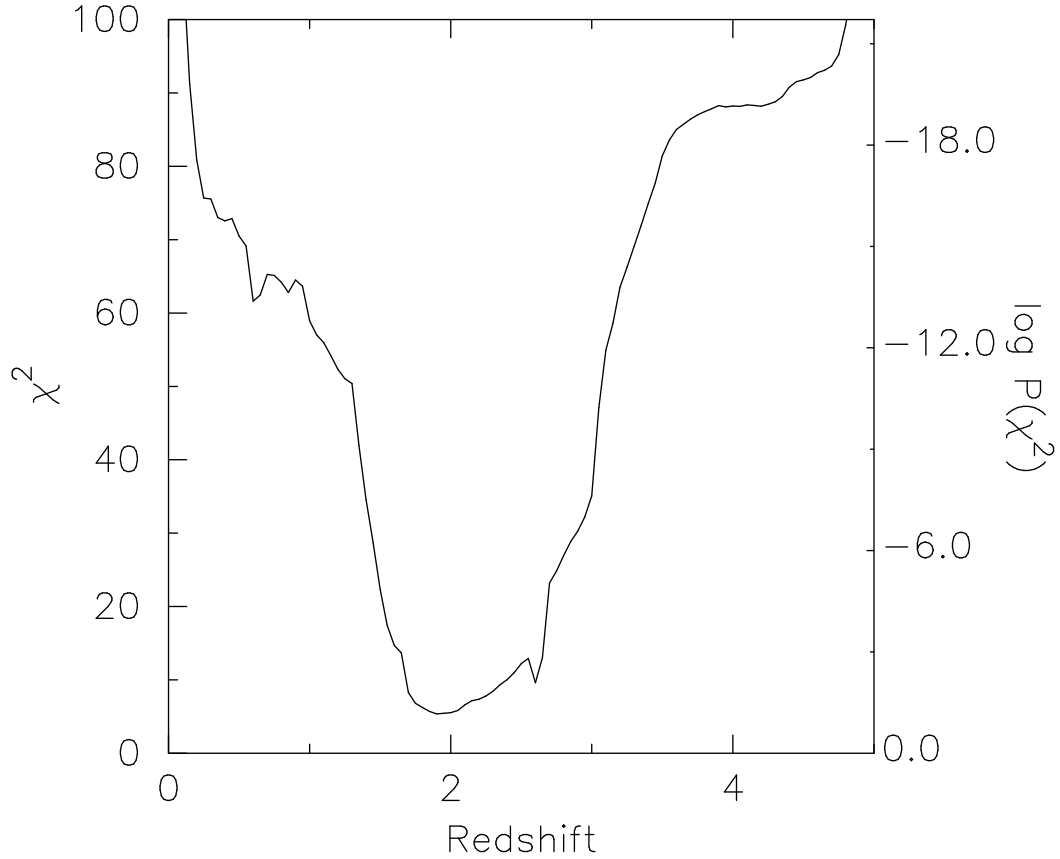


Fig. 6.— χ^2 (left-side y -axis) or logarithm of probability (right-side y -axis) as a function of redshift for the GRB 080325 host galaxy using stellar population synthesis models including emission lines from ionized gas (PÉGASE.2) constructed by Fioc & Rocca-Volmerange (1997) and Fioc & Rocca-Volmerange (1999). A step size of redshift is $\Delta z = 0.05$. At each redshift, a minimum value of χ^2 is adopted among instantaneous burst, exponentially declining ($\tau = 1$ Myr, 10 Myr, 100 Myr, 1 Gyr, and 10 Gyr), and constant SFR models. The best-fit redshift is $z = 1.9$ for $\tau = 1$ Gyr model.

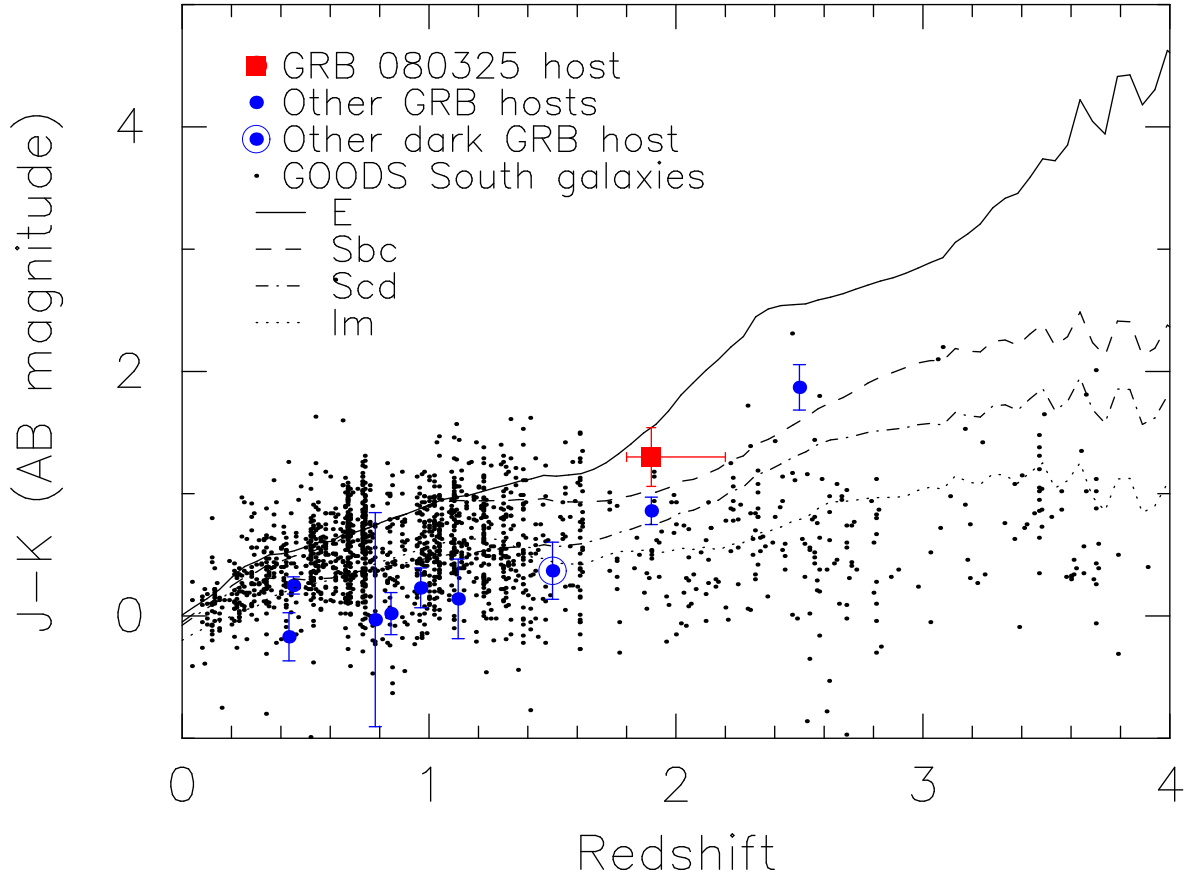


Fig. 7.— $J-K_s$ apparent color in AB magnitude as a function of redshift, for GRB hosts (large blue dots with error bars: Levan et al. 2006; Berger et al. 2007; Jaunsen et al. 2008; Savaglio et al. 2009) and GOODS South galaxies with spectroscopic redshifts (small dots: Grazian et al. 2006). Circled large blue dot shows a dark GRB host defined by optical-to-X-ray spectral index of $\beta_{\text{OX}} < 0.5$ (Zheng et al. 2009). Typical templates of galaxies at $z = 0$ (Coleman et al. 1980) are represented by different line types (elliptical, Sbc, Scd, and irregular types are shown by solid, dashed, dot-dashed, and dotted lines, respectively). Red square corresponds to the GRB 080325 host.

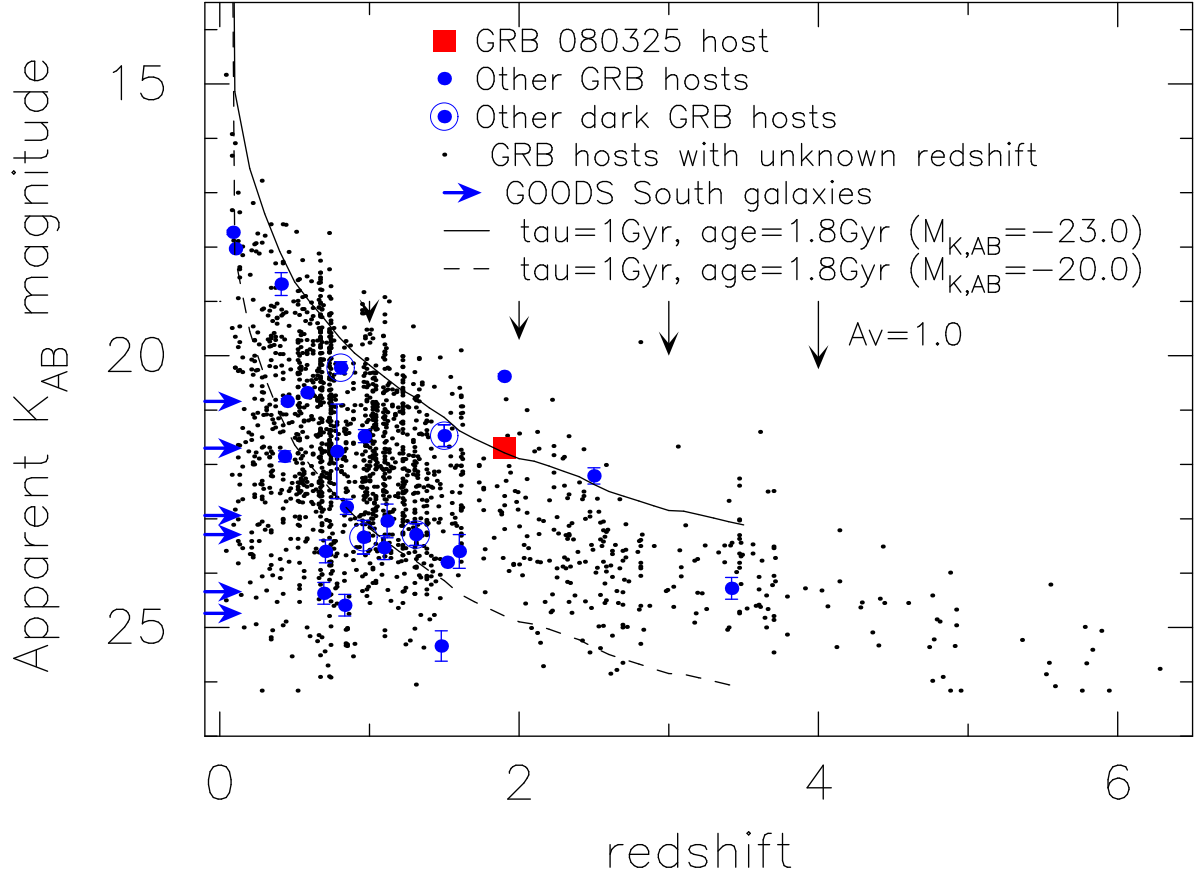


Fig. 8.— Apparent magnitudes as a function of redshift for GRB hosts with and without known redshift (large blue dots and arrows: Chary et al. 2002; Le Floc’h et al. 2003; Levan et al. 2006; Berger et al. 2007; Jaunsen et al. 2008; Tanvir et al. 2008; Savaglio et al. 2009) and GOODS South field galaxies with spectroscopic redshift (small black dots: Grazian et al. 2006). Circled large blue dots show dark GRB hosts defined by optical-to-X-ray spectral index of $\beta_{OX} < 0.5$ (Jakobsson et al. 2004; Zheng et al. 2009; van der Horst et al. 2009). Black arrows are extinction vectors for $A_V = 1.0$ mag at each redshift, given the Calzetti extinction law (Calzetti et al. 2000). Solid and dashed lines show tracks for model galaxies (τ declining models) with $M_K = -23$ and -20 . GRB 080325 host is shown by a red square.

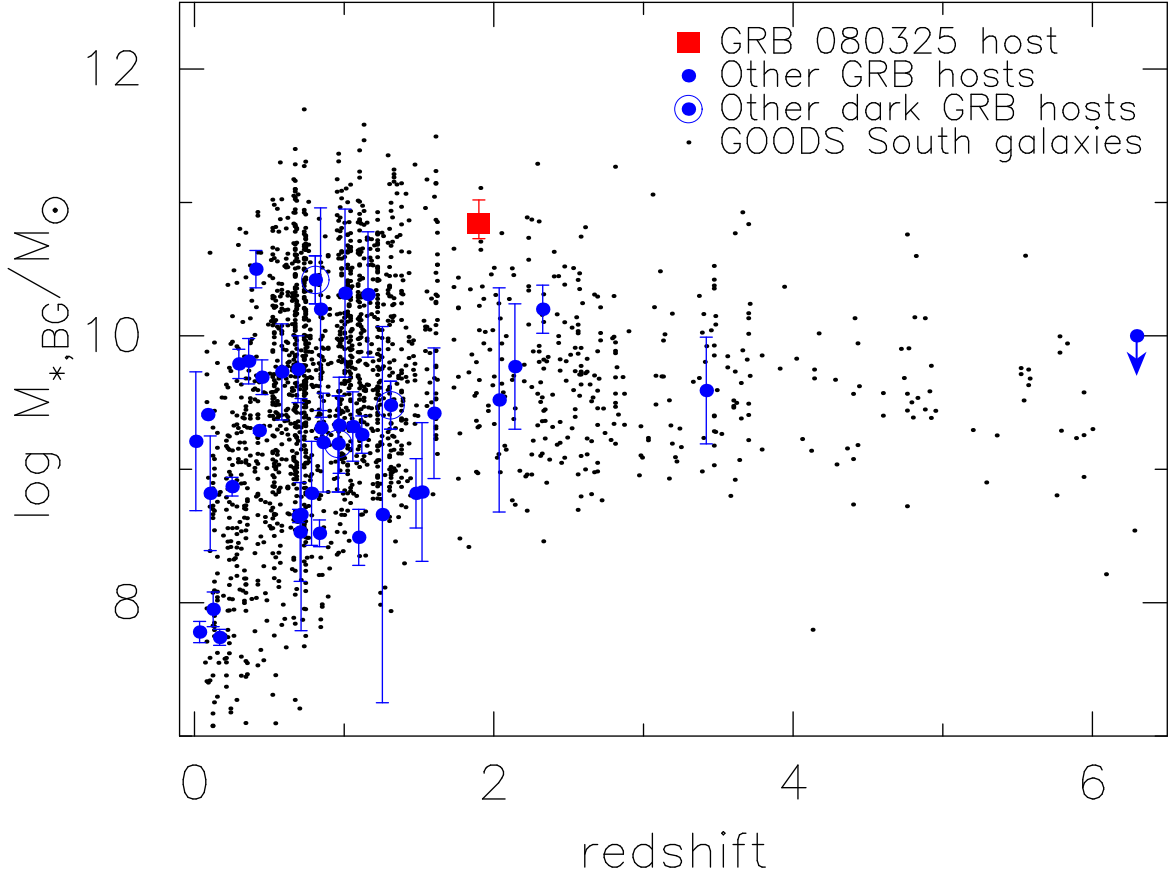


Fig. 9.— Stellar masses derived from the best-fit SED model as a function of redshift for GRB hosts collected by Savaglio et al. (2009) (large blue dots) and GOODS South galaxies by Grazian et al. (2006) (small black dots). Circled large blue dots show dark GRB hosts defined by optical-to-X-ray spectral index of $\beta_{\text{OX}} < 0.5$ (Jakobsson et al. 2004; Zheng et al. 2009; van der Horst et al. 2009). GRB 080325 host is shown with a red square. Stellar masses in this figure are based on Baldry & Glazebrook (2003) IMF, which is adopted for the Savaglio et al. sample.

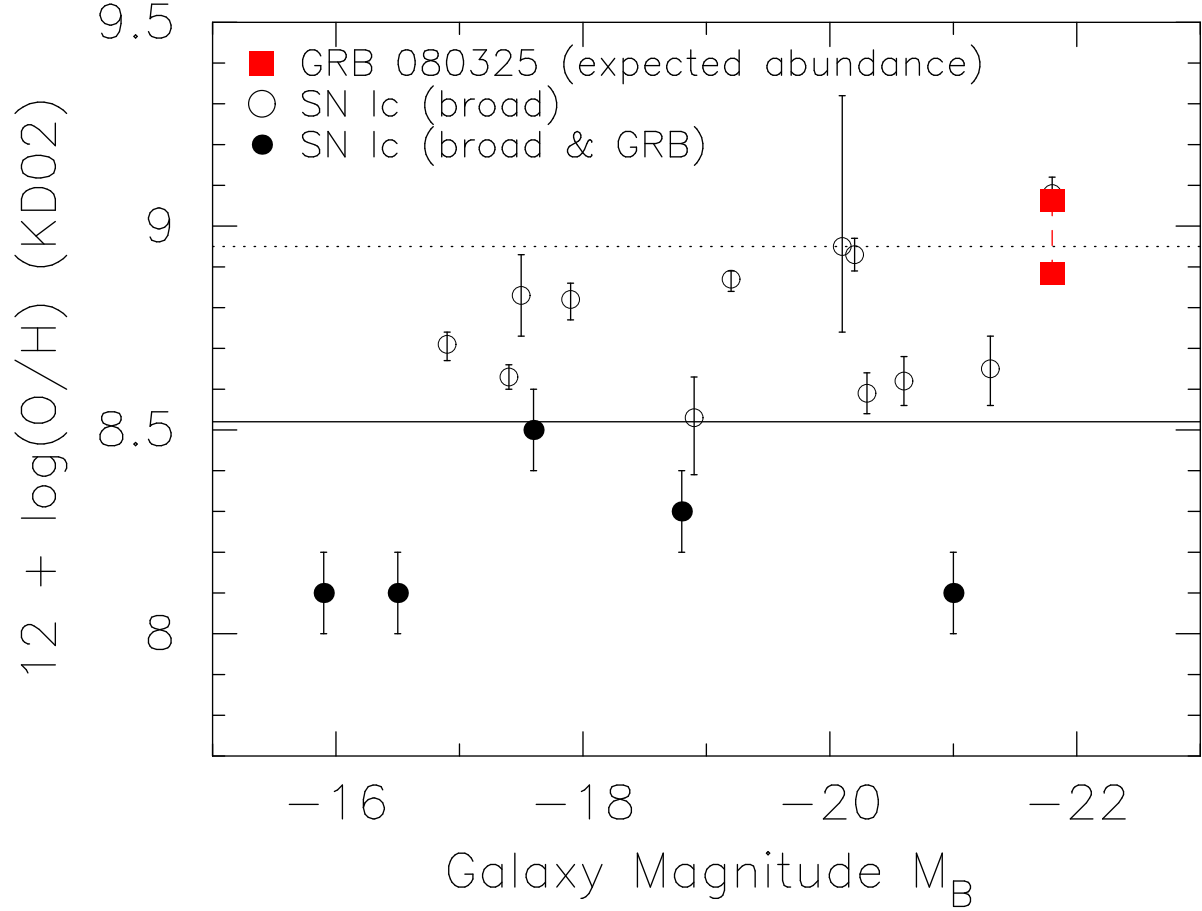


Fig. 10.— Metallicity of the GRB 080325 host, expected from mass-metallicity relations by Erb et al. (2006) and Hayashi et al. (2009) (red squares connected by a dashed line) is compared with the critical metallicity proposed by (Modjaz et al. 2008). Filled circles represent type Ic SNe with GRBs, and open circles are type Ic SNe without GRBs. The critical and solar abundances are shown by solid and dotted lines, respectively. Expected metallicity of the GRB 080325 host is calibrated to Kewley & Dopita (2002) method using conversion coefficients listed in Kewley & Ellison (2008).